

System development of moiré camera array for displacement and strain measurement

Rujika Tuladhar

MSc. Structural Engineering, School of Engineering and Technology, Asian Institute of Technology
Kathmandu, Nepal
rujidear@gmail.com

Dr. Punchet Thammarak

Senior Lecturer, School of Engineering and Technology, Asian Institute of Technology
Pathumthani, Thailand
punchet.thammarak@gmail.com

Abstract—The available conventional sensor like displacement transducer used in Structural Engineering laboratory is expensive. In addition to that, the need of data acquisition device also escalates the expense invested for point contact measurement system. The recent appeal of vision-based measurement technique and search for cost-effectiveness has led to exploration of the established sampling moiré method using cheap CCTV cameras as a viable option. The sampling moiré method is simple and analyzes the displacements from grating images by phase shifting method. A series of trial experiments that were conducted, which demonstrated that the setup is at least as accurate as the more traditional measuring system. An experiment was conducted in a steel I-beam for displacement measurement which has displayed satisfactory result. In addition, the setup was also tested for strain measurement and it has yielded promising result that needs fine tuning. This thesis discusses the challenges, findings and possibility of incorporating vision-based displacement measurement in laboratory platform.

Keywords— Vision-based measurement, Sampling moiré method, CCTV camera, image processing, displacement and strain

I. INTRODUCTION

Vision-based measurement systems present to us fascinating proposition which features simple instrumentation and installation along with remote access yet whole field measurement using a single (camera) sensor. The traditional deformation measurement technologies such as LVDT, strain gage, etc. necessarily require physical access to a structure and are suitable for point measurements only. This interference has led vision-based methods to garner great research interest in recent times [1].

The use of the principle of sampling moiré method [2] for the applicability to the laboratory platform has been explored here. Studies available on the performance of the sampling moiré method are primarily focused on comparing how well the computer simulation [3] [4] and experiments conducted [5] [2] agree with those obtained by displacement sensor. They have highlighted the fact that the method is simple and easy procedure with high accuracy and analysis speed in addition to low-cost performance [6] [7]. There has been development of

the sampling moiré camera for small displacement detection for close-range and long-range displacement measurement [8], which is compact and high resolution but expensive.

Moiré camera is a vision-based, non-contact measurement device in order to analyze the captured images of gratings by image processing technique to measure displacement and strain values in structures. This study focuses to address the implementation and augment the usability of the method for laboratory scale. Several laboratory trials were conducted to characterize the influential factors such as target distance from camera, optimal grating size on measurement performance. This was established by verifying the performance of the sampling moiré method using CMOS sensor-Mars series and then using the scheme for CCTV camera, platform for trials later to be deployed to specimen testing.

The implementation of this scheme could open new doors to supersede the functionality of traditional technology which are otherwise expensive. For example, the cost of the displacement transducer alone is 50K Baht excluding the cost of data logger. Even if 12 units of CCTV cameras, each costing around 2K Baht was used, the overall setup would cost us around 35K Baht. This experiment seeks to make use of vision-based measurement technique and find displacement and strain simultaneously.

II. METHODOLOGY

A. Principle of sampling moiré method

This sampling moiré method is an efficient phase analysis technique that performs analysis of phase distribution on single shot image. In this method, the fundamental principle is illustrated in Figure 1, fringes are gained by “down sampling” from sequential pixels followed by “intensity interpolation” digitally. By phase shifting spatially, i.e., changing start-sampling pixel point in succession such that the sampling interval is similar to the pitch of the specimen grating, series of moiré patterns can be attained. Eventually, from the series of phase shifted moiré patterns, the phase of moiré fringe is analyzed by using the phase shifting method [5] [6] [9] [10] [11].

In Figure 1(h–k), the k-th phase-shifted images can be shown approximately as follows:

$$I_k(i, j) = I_a(i, j) \cos \left[\phi_m(i, j) + 2\pi \frac{k}{N} \right] + I_b(i, j) \quad (1)$$

($k = 0, 1, 2, \dots, N-1$)

where $I_b(i, j)$ represents background intensity in the image,

$I_a(i, j)$ represents the amplitude of the grating intensity and $\phi_m(i, j)$ is the initial phase value of the moiré fringe.

The phase distribution of the moiré pattern can be obtained from frequency 1 of a discrete Fourier

transform (DFT) algorithm or phase-shifting method using Fourier transform (PSM/FT) of Eq. (1). Now, the value of the wrapped phase ϕ for the frequency 1 is represented in equation below.

$$\phi_m(i, j) = -\tan^{-1} \frac{\sum_{k=0}^{N-1} I_k(i, j) \sin \left(k \frac{2\pi}{N} \right)}{\sum_{k=0}^{N-1} I_k(i, j) \cos \left(k \frac{2\pi}{N} \right)} \quad (2)$$

The phase obtained by Eq. (2) is wrapped by 2π lies between $-\pi$ to π which creates discontinuous deformation while calculating. Thus, a phase unwrapping algorithm must be combed by a local phase unwrapping algorithm to ensure accuracy in measurement of strain distribution [12].

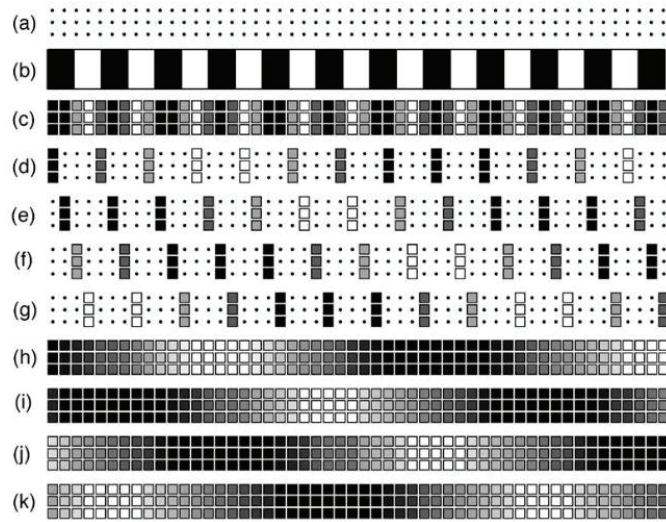


Fig. 1 Phase analysis by sampling moiré method: (a) Sampling points of camera; (b) Specimen grating; (c) Sampled image of Figure (b); (d) Thinned-out image from Figure (c) ($N=4, \alpha=0$); (e) Thinned-out image from Figure (c) ($N=4, \alpha=\pi/2$); (f) Thinned-out image from Figure (c) ($N=4, \alpha=\pi$); (g) Thinned-out image from Figure (c) ($N=4, \alpha=3\pi/2$); (h) Interpolated image of Figure (d); (i) Interpolated image of Figure (e); (j) Interpolated image of Figure (f); (k) Interpolated image of Figure (g) (Adapted from [6])

The phase ϕ_m of the moiré fringe is the subtraction of the phase ϕ_r of the reference grating from the phase ϕ_s of the specimen grating such that:

$$\phi_m(i, j) = \phi_s(i, j) - \phi_r(i, j) \quad (3)$$

The phase ϕ_m of the moiré fringe has to be analyzed while the phase ϕ_r of the reference grating remains unchanged. Thus, the ϕ_s can be calculated as represented in equation below

$$\phi_s(i, j) = \phi_m(i, j) + \phi_r(i, j) \quad (4)$$

The displacement distribution can be derived at by computing the difference of distribution of phase of patterns prior and post deformation. Phase difference ϕ_{m0} and ϕ_{m1} of moiré pattern prior and post deformation are expressed as follows:

$$\phi_{m0} = \phi_{s0} - \phi_r \quad (5)$$

$$\phi_{m1} = \phi_{s1} - \phi_r \quad (6)$$

where ϕ_{s0} and ϕ_{m1} are phases of grating pattern prior and post deformation, respectively. Phase difference $\Delta\phi_s$ of grating patterns prior and post deformation can be found from the difference in phase between ϕ_{m0} and ϕ_{m1} as follows:

$$\Delta\phi_s = \phi_{s1} - \phi_{s0} = \phi_{m1} - \phi_{m0} = \Delta\phi_m \quad (7)$$

(Equations were adapted from [13])

Then, equation (3) was used and the displacement u and strain ϵ of the specimen grating can be obtained in the equations below.

$$u = p \frac{\Delta\phi_m}{2\pi} = -p \frac{\Delta\phi_s}{2\pi} \quad (8)$$

$$\epsilon = \frac{du}{dx} = \frac{p}{2\pi} \frac{d(\Delta\phi_m)}{dx} = -\frac{p}{2\pi} \frac{d(\Delta\phi_s)}{dx} \quad (9)$$

where, p = pitch of the grating.

(Equations were adapted from [10])

B. Instrumentation

The scheme was validated using CMOS sensor-Mars4072S-24uc model (Figure 2 (A)) of sensor size 1/1.7" with pixel resolution of 4000×3000 and frame rate of 24 fps. The camera was directly connected to the computer using USB cable and operated using its software called *icentral* to capture photographs.

For the experiment, Hikvision DS-2CE16D0T-IRF HD 1080P IR bullet camera (CCTV camera), 2 Megapixel high performance image sensor of 6mm lens and video frame rate of 25 fps, was used to capture video for the scheme. The videos were recorded in the DVR box and exported for further processing as shown in Figure 2 (B) and (C).



Fig. 2 Photographs (A) CMOS sensor, (B) CCTV camera, (C) DVR box

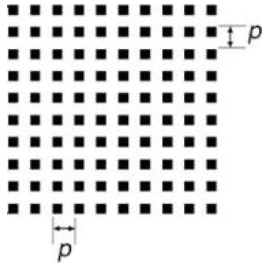


Fig. 3 2-D Grating ([2])

Similarly, 2-D gratings of 4mm, 2mm and 1mm pitch were used as in sample Figure 3. The grating used for measurement requires constant pitch and sharp variation of contrast. Initially, gratings printed on normal A4 paper using laser printer were used and later they were printed on 4"x3" matte photograph paper and finally upgraded to gratings printed at Amarin Printing & Publishing Public Company Limited, publishing house, with 300 dpi on matte art paper by using digital printing technique.

The Matlab code was developed using the phase analysis method, required captured grating photographs as input. The phase difference of the grating before and after deformation provided the displacement values. The procedure of which has been illustrated in Figure 4.

The sampling pitch in pixel, and the position of pixel at which the displacement are the input values used for processing. The sample pitch was counted by observing the pixels that make up one pitch in the photograph.

C. Basic Setup

The general setup was such that the linear guide was used for displacing the grating. The grating, held inside acrylic holder, was mounted on a linear guide secured by tape over the moving stage of the guide. This setup was arranged such that the grating was illuminated using two 50W LED flood light. The amount of displacement was controlled by the displacement transducer which was connected to a data logger. The moving stage was displaced at certain intervals like 1mm and 0.5mm in translation in x-direction and to and fro motion using displacement transducer.

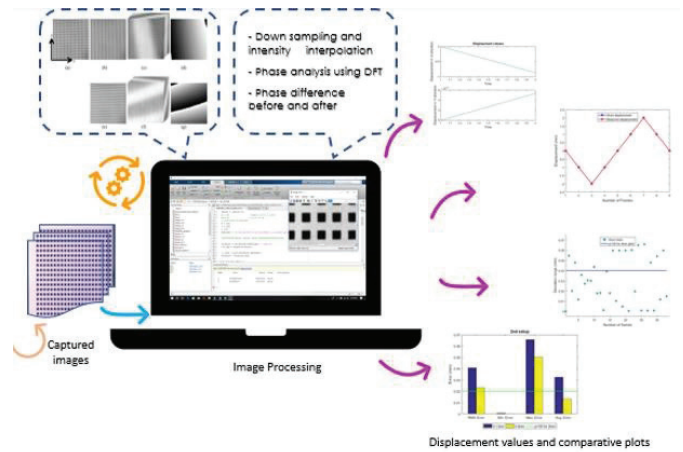


Fig. 4 Diagram of image processing of the captured images

D. Trial experiments using CMOS sensor

First, the suitability of the scheme was established with a series of trial experiments performed using CMOS sensor Mars and gratings of 4mm and 2mm pitch.

The first trial with short tripod and A4 printed grating and the second trial with long tripod and matte photograph grating, were displaced at intervals of 1mm to 0.25mm for various cases. By corresponding the displacement values given to that of measured using the code, the credibility of the code was assured.

E. Trial experiments using CCTV camera

16 cases were trialed for 3 setups with 4mm, 2mm and even 1mm pitch grating to determine a suitable pitch and distance for the experiment. The linear guide was displaced up to double the pitch in one direction and equal to the pitch in both directions for the experiment. The camera setups were maintained throughout the trials at distances of 5cm, 10cm and 15cm for 4mm and 2mm pitch while at distance 5cm and 10cm for 1mm pitch from the grating panel. The trials differed in the improvements in the camera settings, the grating being the upgraded matte art one.

All in all, 4mm and 2mm pitch seemed to deliver consistent outcome and the distance 10mm or less seemed to work better while with 1mm pitch, the deviation values under the theoretical band of error was not achieved for all cases. The theoretical band of error is the $p/100$ th of the grating pitch for this method.

III. EXPERIMENT CONDUCTED ON THE SPECIMEN

The specimen used in the experiment is a steel I-beam which is 1170mm long. The span between the two supports was 1000mm. The total height and width of the beam was 150mm each. The web was 7mm thick while the flange was 10mm thick.

A. Experimental setup

A symmetric three-point bending test was performed on the specimen to measure the deflection at the point of loading and

determine the strain values. The displacement transducers were located at the bottom flange of the beam at a distance of $L/4$ th of the span along the span as seen in Figure 5. The gratings were also pasted on wooden panels at the same positions facing the array of three cameras. Eight strain gages were installed such that four of them were laid on either side of the mid span between the $L/4$ th positions as shown in Figure 6. The specimen was loaded at the mid of the beam by the loading frame of 15 tons capacity.

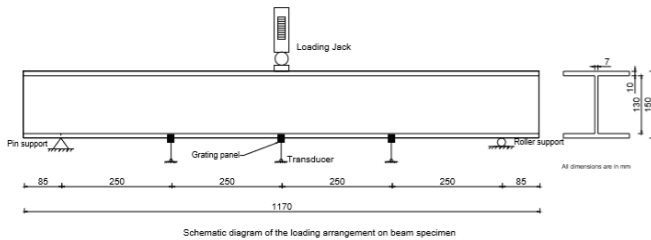


Fig. 5 Schematic diagram of the experiment

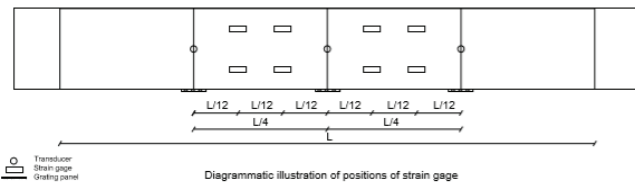


Fig. 6 Schematic designs of the instruments on the beam

In the experiment, Figure 7, 4mm and 2mm gratings were used to capture the x-direction and y-direction displacement simultaneously from the array of cameras. The CCTV cameras were kept at 10cm distance from position A and position C and at 5cm distance from position B. The specimen was pre-loaded at 1 ton at the center of top flange of the specimen with the load cell at every 0.5 tons interval up to 8 tons and unloaded back to pre-loaded position. The displacement values were analyzed at the pixel at which $L/4$ th position of the specimen was marked on the grating panel as seen in Figure 8.



Fig. 7 Photograph of the experiment setup in specimen with labels. 1) Loading cell, 2) I-beam Specimen, 3) Grating panel, 4) Linear guide, 5) CCTV camera, 6) Monitor for operating the camera, 7) DVR box, (A, B, C) Camera positions

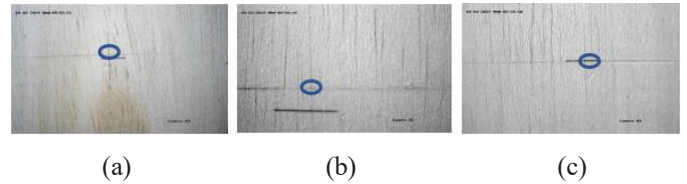
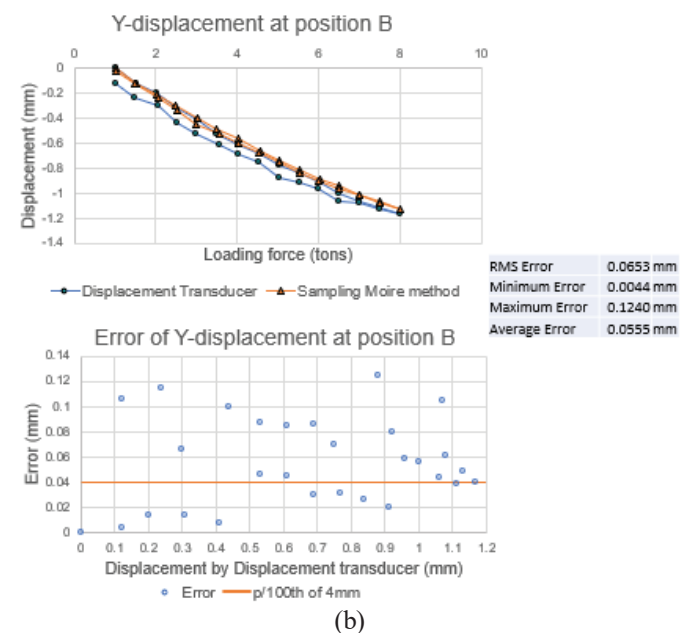
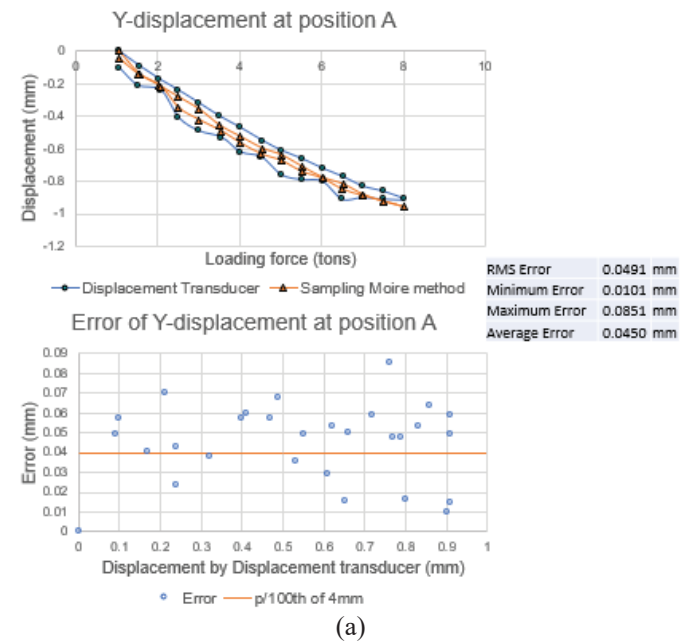


Fig. 8 Photographs showing the pixel position (Column, Row) at which the analysis was done for cameras. (a) at A (433, 233), (b) at B (335, 374), (c) at C (542, 256)

B. Displacement measurement



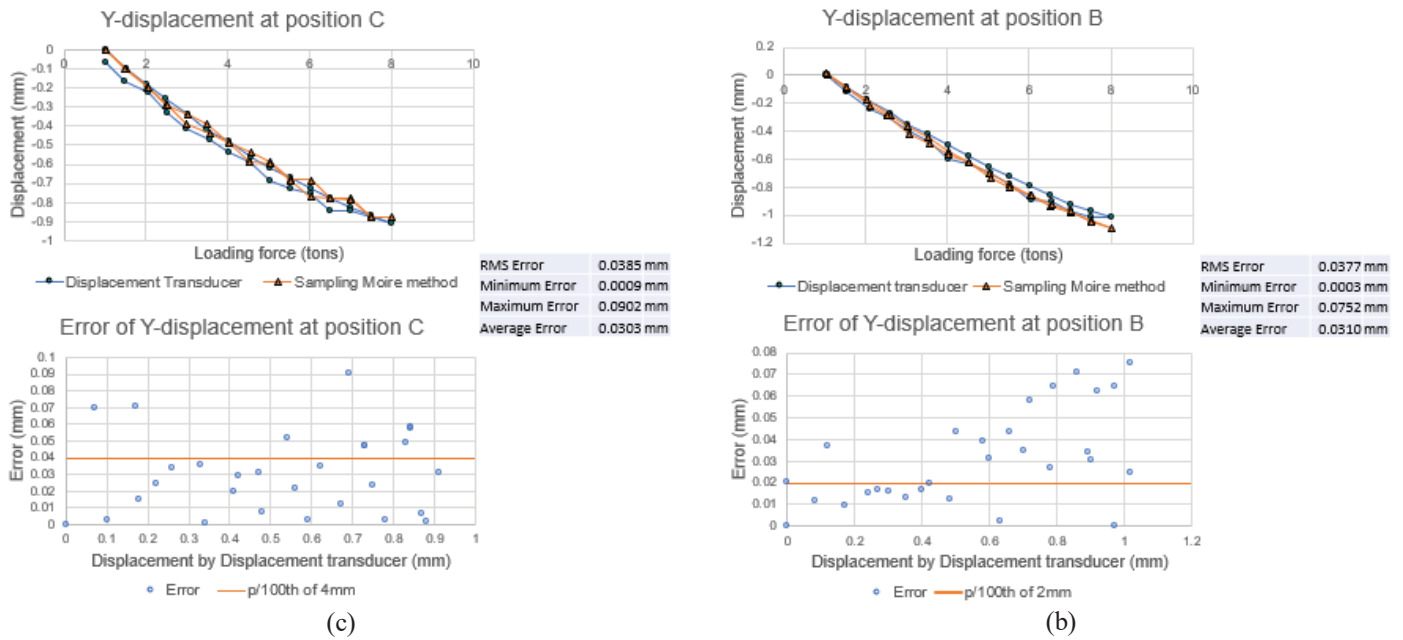


Fig. 9 Various graph plots for displacement values by displacement transducer and the sampling moiré method and their derivatives at camera position (a) A, (b) B and (c) C respectively for 4mm grating

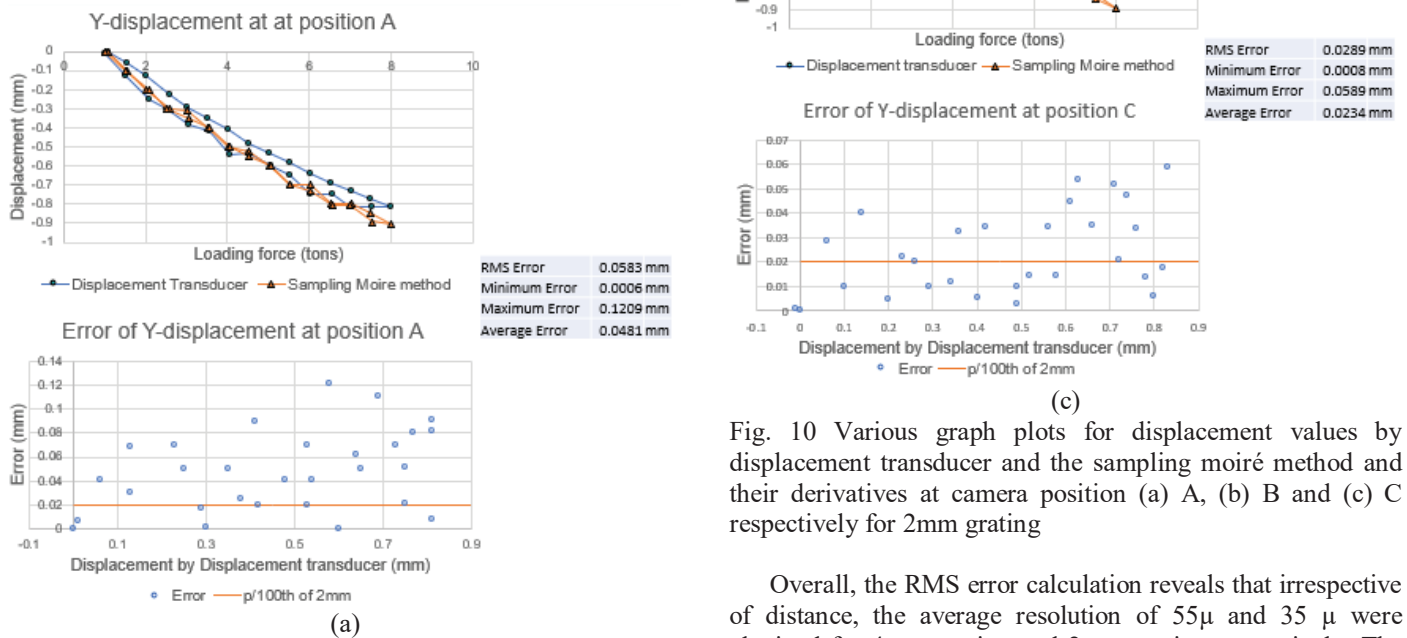


Fig. 10 Various graph plots for displacement values by displacement transducer and the sampling moiré method and their derivatives at camera position (a) A, (b) B and (c) C respectively for 2mm grating

Overall, the RMS error calculation reveals that irrespective of distance, the average resolution of 55μ and 35μ were obtained for 4mm grating and 2mm grating respectively. The first graph for each position from Fig. 9 and 10 show us how the displacement values are varying over loading and unloading by both the methods. While, the second graph for each position from Fig. 9 and 10 show the variation of error values that are within the $p/100$ th of grating pitch and the ones that exceed.

C. Strain measurement

Strain is the deformation incurred in a solid when stress is produced on it due to application of force. Therefore, strain is the amount of deformation per unit its original length.

$$\text{Here, Strain } (\epsilon) = \frac{\text{relative change in } x\text{-displacement } (\Delta l)}{\text{gauge length } (L_0)}$$

Strain gages of gauge length 5mm and resolution $1 \mu\epsilon$ were installed at locations as seen in Figure 6. Thus, 2.5 cm gauge length (this case), would require 0.025μ resolution for displacement measurement. If p/100th of grating was taken to be 0.025μ , the size of grating would be 2.5μ which is way smaller and would require nano-printing of the grating pitch.

D. Outcome of the measurement scheme and its limitation:

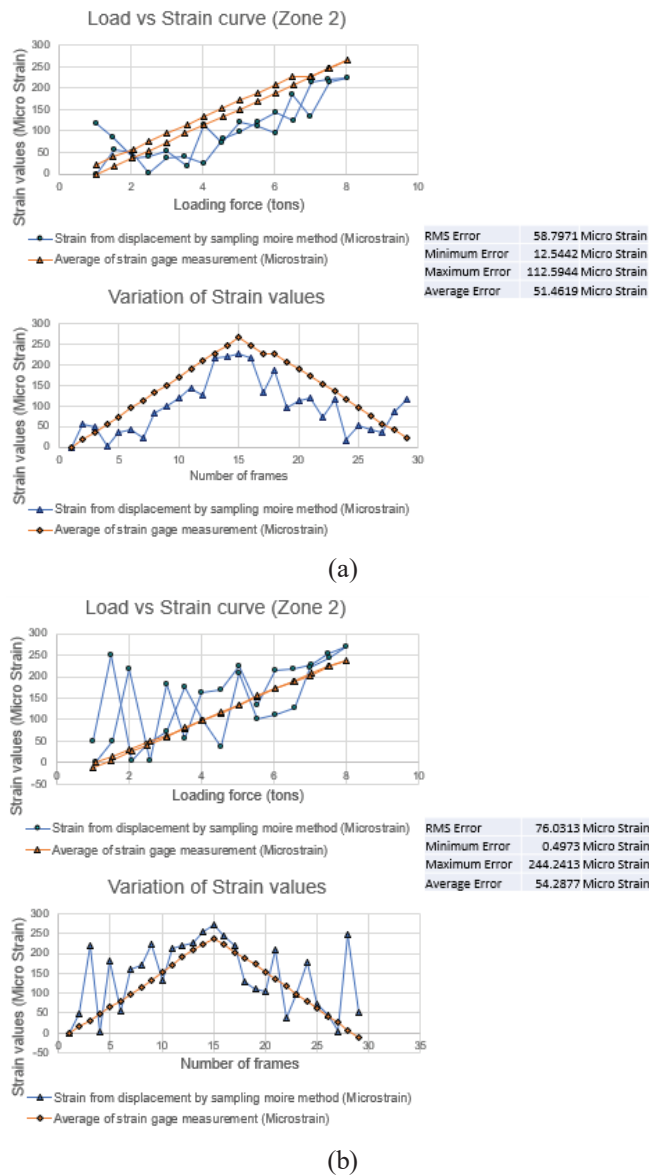


Figure 11 Various graph plots for strain values by strain gage and the sampling moiré method and their derivatives for Zone 2 using (a) 4mm grating and (b) 2mm grating respectively

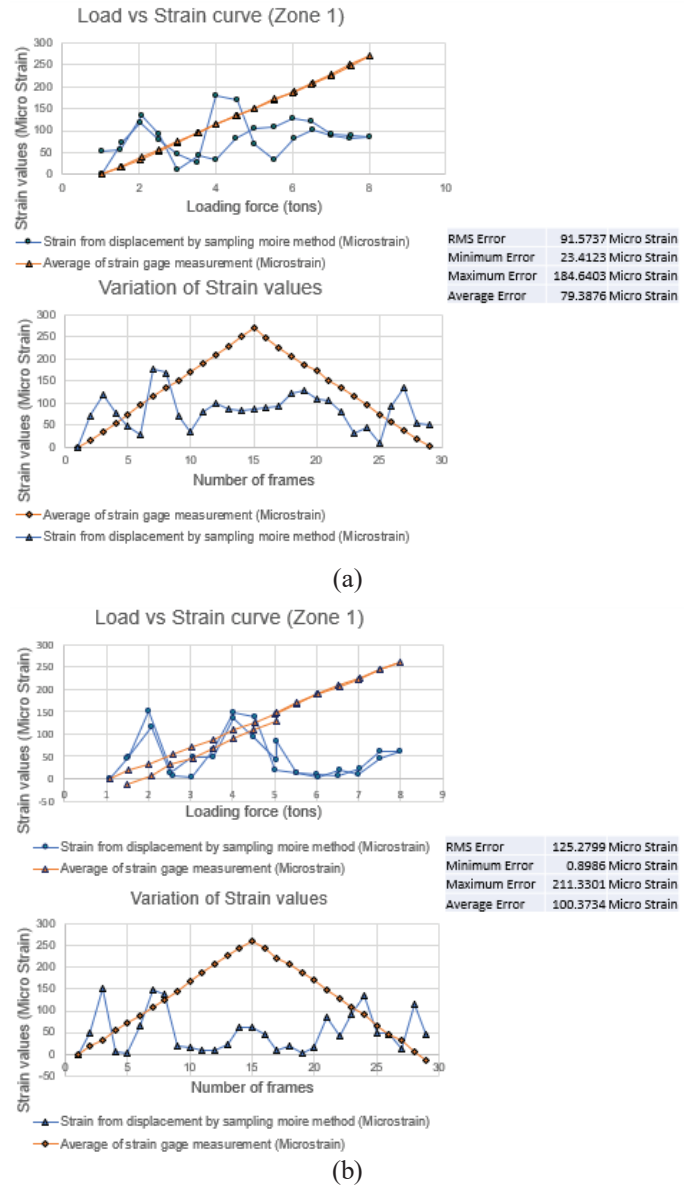


Fig. 12 Various graph plots for strain values by strain gage and the sampling moiré method and their derivatives for Zone 1 using (a) 4mm grating and (b) 2mm grating respectively

Taking conservative approach, even if fluctuation of 10% of the maximum strain is allowed, 0.25μ resolution is needed, which is still small. The inherent amount of error in the current scheme is $186 \mu\epsilon$. In the results, the x-displacement is towards left and thus all the values tend to be negative otherwise and the plot henceforth are done taking solely magnitude.

The average of strain gage values seems to agree better through both conditions for Zone 2 and lags for loading condition for Zone 1. However, the calculated strain values do not follow the pattern of the averaged ones for either Zone as seen from the third figure of the graphs. From the second graph in each Fig. 11 to 12, it is seen that Zone 2 captured the tentative pattern better as is evident from R-squared value of 4mm grating. All things considered, the RMS Error has not

been exceeded from the error of the measurement scheme of $186\text{ }\mu\text{ε}$.

E. Comprehensive summary

In specimen experiment, 4mm grating pitch has yielded better results for both y-displacements and strain values calculated. The average resolution is found to be $50\text{ }\mu$ for 4mm grating pitch and $40\text{ }\mu$ for 2mm grating pitch on the liberal side. Observation has revealed that the resolution of displacement transducer along with data logger fluctuates $10\text{ }\mu$ in unloaded condition and up to $40\text{ }\mu$ when the sensor is loaded for a certain time. Considering the setup that was not devoid of number of factors that could affect the calculations, the displacement measurement is satisfactory for laboratory conditions.

As far as strain measurement is concerned, Zone 2 has captured the progression of strain to some extent. It has demonstrated that strain measurement is possible by the moiré measurement scheme with improvement in resolution.

IV. DISCUSSIONS

The sampling moiré method originally proposed by (Morimoto & Fujigaki, 2009) was assessed for displacement measurement through a series of tests conducted using CMOS sensor to establish the efficacy of the method. Further, the same tests were conducted with CCTV camera to examine if the results were reproducible. Finally, an experiment was conducted on specimen by loading to obtain displacements in both directions and calculating strain from x-displacement.

We can conclude that this method is promising visual displacement measurement technique for Structural Engineering Laboratory by using CCTV cameras. It displays adequate performance unaffected by input voltage and temperature changes unlike other traditional sensors. Low-cost, low resolution CCTV cameras have adequate resolution to perform consistently which is preferable. Strain measurement is also viable from this measurement scheme as is evident from the above results with improvements

There are some inherent constraints in the moiré scheme that has to do with both grating and the camera. In case of grating, the quality of printing is critical. Even with 300 dpi digital printing technique, the best that could be procured, there exist inconsistencies in the printing which is evident when the camera is close to the specimen. Similarly, a CCTV camera has a limited usable area coverage for analysis due to its wide-angle lens. In this case, only a circular area at center with radius of 1/4th of the width of a frame is at dispose. Likewise, for short gage length issue, the displacement resolution of $55\text{ }\mu$ from available measurement scheme to achieve $7\text{ }\mu$ resolution as calculated above for strain measurement from current setup up is indeed challenging. For this, an immense improvement of about 7 times the current resolution is required.

The recommendations for further improvement in the scheme would be to resolve the issue of the printing quality of grating pattern optimized over the resolution sought. Also, exploring the strain measurement by the scheme by improving the resolution, adjusting the gage length, etc. Furthermore,

upgrading the physical video retrieval system as of now to real-time displacement measurement could be a prominent scope for laboratory platform.

REFERENCES

- [1] Yan, X., & Brownjohn, J. M. W. (2018). Vision-based systems for structural deformation measurement: case studies. <https://doi.org/10.1680/jstbu.17.00134>
- [2] Ri, S., Fujigaki, M., & Morimoto, Y. (2010). Sampling Moiré Method for Accurate Small Deformation Distribution Measurement. *Experimental Mechanics*, 50(4), 501–508. <https://doi.org/10.1007/s11340-009-9239-4>
- [3] Ri, S., & Muramatsu, T. (2012). Theoretical error analysis of the sampling moiré method and phase compensation methodology for single-shot phase analysis. *Applied Optics*, 51(16), 3214–3223. <https://doi.org/10.1364/AO.51.003214>
- [4] Ri, S., Muramatsu, T., & Saka, M. (2011). A Phase Compensation Technique of Sampling Moiré Method for Accurate Single-Shot Phase Analysis. *Applied Mechanics and Materials*, 70, 243–248. <https://doi.org/10.4028/www.scientific.net/AMM.70.243>
- [5] Morimoto, Y., & Fujigaki, M. (2011). Theory and Application of Sampling Moiré. In *Recent Advances in Mechanics* (pp. 227–248).
- [6] Morimoto, Y., & Fujigaki, M. (2009). Accuracy of sampling moiré method. *Proceedings of SPIE - The International Society for Optical Engineering*, 7375(d), 2–7. <https://doi.org/10.1117/12.839206>
- [7] Ri, S., Muramatsu, T., Saka, M., Nanbara, K., & Kobayashi, D. (2012). Accuracy of the Sampling Moiré Method and its Application to Deflection Measurements of Large-Scale Structures. *Experimental Mechanics*, 52(4), 331–340. <https://doi.org/10.1007/s11340-011-9491-2>
- [8] Nakabo, M., Fujigaki, M., Morimoto, Y., Sasatani, Y., Kondo, H., Hara, T., ... Wakayama, S. (2011). Development of Sampling Moire Camera for Landslide Prediction by Small Displacement Measurement. In *Conference Proceedings of the Society for Experimental Mechanics Series* (Vol. 5, pp. 323–330). <https://doi.org/10.1007/978-1-4614-0228-2>
- [9] Ri, S., & Muramatsu, T. (2010). A simple technique for measuring thickness distribution of transparent plates from a single image by using the sampling moiré method. *Measurement Science and Technology*, 21(2), 025305. <https://doi.org/10.1088/0957-0233/21/2/025305>
- [10] Fujigaki, M., Sasatani, Y., Masaya, A., Kondo, H., Nakabo, M., Hara, T., ... Kurokawa, N. (2011). Development of Sampling Moire Camera for Real-Time Phase Analysis. *Applied Mechanics and Materials*, 83, 48–53. <https://doi.org/10.4028/www.scientific.net/AMM.83.48>
- [11] Ri, S., Numayama, T., Saka, M., Nanbara, K., & Kobayashi, D. (2012). Noncontact Deflection Distribution Measurement for Large-Scale Structures by Advanced Image Processing Technique. *Materials Transactions*, 53(2), 323–329. <https://doi.org/10.2320/matertrans.L-M2011852>
- [12] Wang, Q., Ri, S., Tsuda, H., & Koyama, M. (2018). Optical full-field strain measurement method from wrapped sampling Moiré phase to minimize the influence of defects and its applications. *Optics and Lasers in Engineering*, 110(May), 155–162. <https://doi.org/10.1016/j.optlaseng.2018.05.020>
- [13] Nakabo, M., Fujigaki, M., Morimoto, Y., Sasatani, Y., Kondo, H., Hara, T., ... Wakayama, S. (2011). Development of Sampling Moire Camera for Landslide Prediction by Small Displacement Measurement. In *Conference Proceedings of the Society for Experimental Mechanics Series* (Vol. 5, pp. 323–330). <https://doi.org/10.1007/978-1-4614-0228-2>